JTTEE5 14:134-140
DOI: 10.1361/10599630522684
1059-9630/$19.00 © ASM International

Peer Reviewed

Protection of Ti6Al4V Surfaces by Laser Dispersion of Diborides

Andreas Wank, Bernhard Wielage, Harry Podlesak, Klaus-Jürgen Matthes, and Gerald Kolbe

(Submitted January 5, 2004)

In this work, one- and two-step laser dispersing of Ti6Al4V surfaces by use of elemental boron (B) as well as TiB_2, ZrB_2, and CrB_2 was carried out with CO_2 and Nd:YAG lasers using an adapted apparatus to provide inert conditions. Depending on the laser system, melt pool depths between 200 µm and more than 1000 µm were achieved, and the boride precipitates allowed an increase of the surface hardness from 350 $HV_{0.05}$ in the initial state to more than 600 $HV_{0.05}$. The modified surface areas were characterized by means of optical microscopy, scanning electron microscopy, and EDXS. Oscillating and cavitation erosion wear tests were carried out. For reinforcement of component surfaces with complex shape, a two-step laser deposition process and a technology for predeposition of diboride layers with defined thickness is required. The applicability of vacuum plasma spraying for predeposition is discussed.

Keywords boride, laser treatment, Ti-6Al-4V, TiB_2, wear protection

1. Introduction

Despite their high price, titanium (Ti) alloys are widely used in industries owing to their outstanding high specific strength and excellent corrosion resistance, but the low wear resistance reduces their applicability. Therefore, substantial research has been carried out on the wear protection potential of different surface modification and coating processes. Physical vapor deposition (PVD) and chemical vapor deposition (CVD) processes can produce extremely hard coatings, but due to their low hardness, titanium alloys cannot provide good support, which results in coating spallation or cracking when high local load is applied on a component surface in use. For example, electron beam-physical vapor deposition (EB-PVD) TiN coatings provide excellent tribological properties at moderate load, but fail if a thickness depending load threshold is exceeded (Ref 1, 2). The demanded high process temperatures and long processing times for CVD diamond coating deposition result in strong adhesion due to the formation of a TiC layer at the interface, but also provoke intolerable microstructure changes of the Ti alloy (Ref 3-5). The concomitant of embrittlement by hydrogen absorption can be overcome by a subsequent heat treatment in vacuum (Ref 6, 7).

Conventional thermally sprayed wear protective coatings do not exhibit the outstanding corrosion properties of Ti alloys. However, reactive plasma spraying, both in controlled atmosphere and by use of a nozzle extension, in which inert shielding gases are fed along with the reactive gases, flanged to the nozzle of a plasma torch operating at ambient conditions, permits the production of Ti coatings with high hard phase content (Ref 8-10). Nitriding has been proven to be more effective than carburizing, permitting nearly full conversion of the titanium forming Ti_2N, which results in hardness values up to 900 $HV_{0.3}$. The hardness increase is not only due to the formation of hard nitride phases but also to a solid nitrogen solution in Ti lattice (Ref 11). The wear resistance increases significantly. Investigations concerning the corrosion resistance and lifetime of coated Ti alloy components under dynamic load have not yet been carried out. It is likely that the decreased ductility of the coatings results in eased crack initiation and growth.

Besides coating processes, surface modification processes have been applied to improve the wear protective properties of titanium alloy surfaces. By a thermochemical treatment in nitrogen-rich atmosphere, a few-micrometers-thin hard TiN_x boundary layer is formed. Underneath a diffusion zone of about 100 µm thickness is generated and provides support to the TiN_x layer. The zone contributes in significantly improved wear resistance even at high load. However, the long heat treatment (>10 h) at temperatures ranging between 650 and 800 °C also results in microstructure changes of the treated components core (Ref 12, 13). Additionally, the embrittlement in the diffusion zone due to dissolution of nitrogen eases crack initiation and therefore decreases the lifetime of a component under cyclic load.

Laser gas nitriding permits obtaining greater thicknesses (~500 µm) of the hardened surface area and local processing (Ref 14, 15). For high nitrogen concentrations in the melt pool, the evolution of a dendritic TiN_x phase is observed. High content of this phase results in hardness values of 1000 $HV_{0.1}$ and significantly improved wear resistance. However, the dendritic type of TiN_x phase also decreases the component lifetime under cyclic load.

The original version of this article was published as part of the ASM Proceedings, *Thermal Spray 2003: Advancing the Science and Applying the Technology, International Thermal Spray Conference* (Orlando, FL), May 5-8, 2003, Basil R. Marple and Christian Moreau, Ed., ASM International, 2003.

Andreas Wank, Bernhard Wielage, and **Harry Podlesak,** Institute of Composite Materials, Chemnitz University of Technology, 09107 Chemnitz, Germany and **Klaus-Jürgen Matthes,** and **Gerald Kolbe,** Institute of Welding Technology, 09107 Chemnitz, Germany. Contact e-mail: andreas.wank@wsk.tuchemnitz.de.

Considering the individual drawbacks of each presently applied coating or surface modification technology, there is need for a process that improves the wear resistance of Ti alloy surfaces without negative influence on the corrosion resistance or lifetime under cyclic load. This can be achieved by embedding of corrosion-resistant hard phases in Ti alloy matrices without decreasing the matrix ductility. Embedding of TiB_2 or ZrB_2 in Ti alloy matrices seems to be capable of reaching this goal due to the negligible solubility of boron (B), in Ti in solid state (Fig. 1). Therefore, even if parts of the diborides are molten and/or dissolved in the Ti alloy melt during processing, precipitation during solidification of the melt will result in formation of hard boride phases again and the metallic Ti alloy matrix will remain ductile (Ref 16).

This concept can be used for thermal spray applications by use of composite feedstock with Ti alloy matrix and diboride reinforcement. Generally, vacuum plasma spraying is favorable, as the inert environment prohibits decreased ductility of the Ti matrix due to reactions with oxygen or nitrogen. Previous investigations proved the applicability of vacuum plasma spraying even for production of pure diboride coatings (Ref 18, 19). In contrast, atmospheric plasma spraying with and without application of inert gas shrouds generally results in high oxide contents (Ref 20). Thermal spray coatings show the drawback of limited adhesion strength. This drawback can be overcome by laser dispersing. One-step and two-step laser deposition processes can be applied. The latter is less cost efficient, as a further process step needs to be carried out, but the demands to achieve inert conditions in the processed area are easier to fulfill. Both processes were used for reinforcement of Ti alloy surfaces.

2. Experimental

Ti6Al4V was chosen as an exemplary alloy, as it is the most popular among the Ti alloys. This alloy has a close-packed hexagonal α-phase and a β-phase with body-centered-cubic crystal structure. Investigations were carried out with Ti6Al4V sheets with the dimension $100 \times 100 \times 10\ mm^3$ and $150 \times 100 \times 10\ mm^3$.

The preparation of the surface is important for a high-quality laser treatment. After roughening up the surface by corundum blasting and a subsequent ultrasonically assisted cleaning process applying acetone, an etching process using an aqueous solution of a mixture of HNO_3 and HF (pickling paste SARTOX) was carried out. The roughened surface allows good absorption of the laser energy.

Laser treatment was carried out with a 1.7 kW CO_2 laser (Rofin Sinar 1700 RF), a 3.5 kW CO_2 slap laser (Rofin Sinar DC 035), and a 4.4 kW Nd:YAG laser (Rofin Sinar DY 044) (Hamburg, Germany). The process parameters are shown in Table 1 and a sketch of laser processing is given in Fig. 2.

For laser alloying by addition of elemental B, the pastes with ethanol as fast vaporizing binder were applied to achieve a homogeneous covering of the prepared Ti6Al4V surfaces prior to laser treatment. The B powder improved laser energy absorption, which resulted in deeper remelting depth in comparison to that achieved by clean surfaces.

For laser dispersion by one-step laser deposition, powders were fed in an inert carrier gas stream by a conventional thermal spray powder feeder. The evolving dust of the powders partially absorbed the laser beam and contaminated the optical mirrors. Both caused a decreased remelting depth. To protect the re-

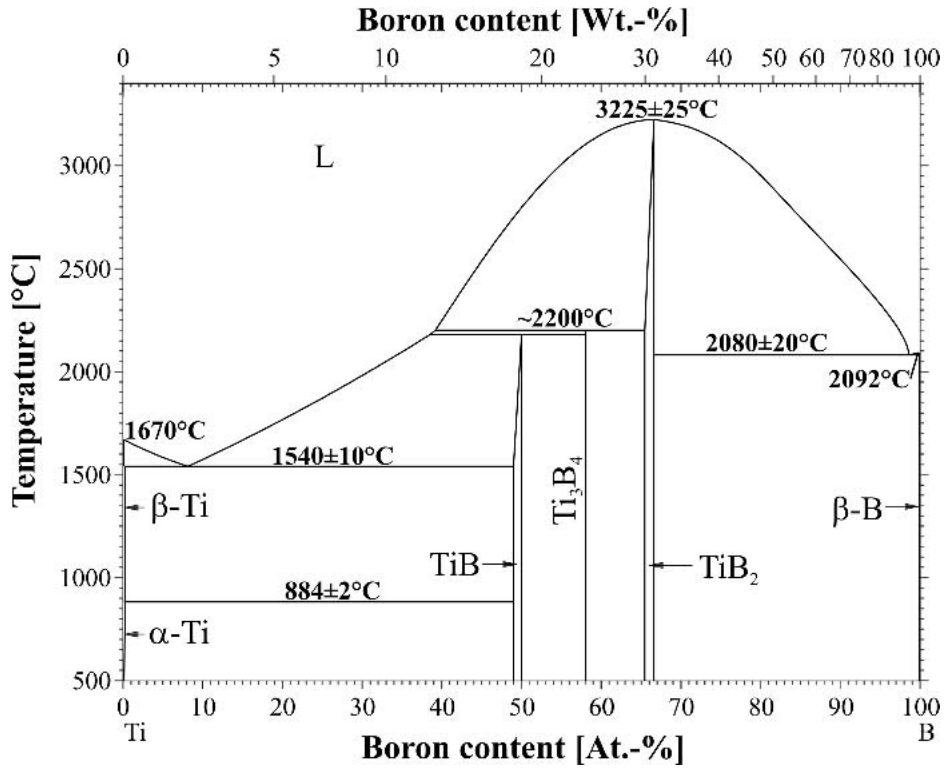

Fig. 1 TiB phase diagram (Ref 17)

melted zone against oxidation, a shield gas protection using argon was installed. However, due to the complex interaction of shield gas, carrier gas and environment air entrainment by turbulences cannot be prohibited completely. Therefore a special setup protecting the molten zone down to a temperature of 300 °C by an inert shield gas (Ar, He, or Ar/He mixtures) was designed (Ref 21). Additionally, the optical mirrors and the very sensitive zinc-selenide window were protected by a coaxial inert gas flow inside the setup.

In addition to the conventional laser dispersion by one-step laser deposition, the applicability of pastes with different binders for two-step laser deposition was tested. Besides ethanol, vaseline, polyvinyl alcohol (PVA), and polyethylene glycol (PEG) were applied. Prior to laser treatment the binder was removed by thermal treatment. The degree of laser track overlapping was optimized. Amorphous elemental B powder and water-washed TiB_2, ZrB_2, and CrB_2 powders with different powder size fractions were applied (Table 2). The powders were supplied by Wacker Ceramics GmbH, Kempten, Germany.

The microstructure of the laser treated surfaces was characterized using optical microscopy, scanning electron microscopy (SEM) (LEO 1455VP, Cambridge, UK) and energy-dispersive x-ray microanalysis (EDXS) (EDISON, GETAC GmbH, Maine, Germany). For detection of B in the formed phases, the accelerating voltage of the electron beam was reduced to 5 keV. Additionally, the local microhardness was determined.

The wear resistance was investigated by means of an oscillating and a cavitation erosion wear test. Schemes of the tests are given in Fig. 3. Specimens were subject to the oscillating wear test in polished surface state ($R_z \leq 1$ µm) using counterbodies of hardened steel 100Cr6 and alumina balls of 10 and 9 mm diameter, respectively. The oscillating frequency was 20 Hz and the amplitude equal to 1 mm. Load levels of 5 and 20 N were applied, and the testing was carried out for durations of 15 and 60 min. Cavitation erosion tests (ASTM G 32-92) were carried out in indirect mode using distilled water as environment. The frequency of the sonotrode working at a power of 2 kW and amplitude of 50 µm was 20 kHz. The water temperature was kept constant at 25 °C, and the specimens were mounted at a distance of 0.5 to 0.7 mm to the sontrode surface.

The influence of the surface modification by laser dispersion of diborides on the electrochemical corrosion behavior was characterized by potentiodynamic polarization measurements according to the German standard DIN 50,918. Both 0.6 mol NaCl and 0.5 mol H_2SO_4 solutions were applied.

First experiments concerning the manufacturing of diboride coatings on Ti6Al4V substrates by vacuum plasma spraying were carried out.

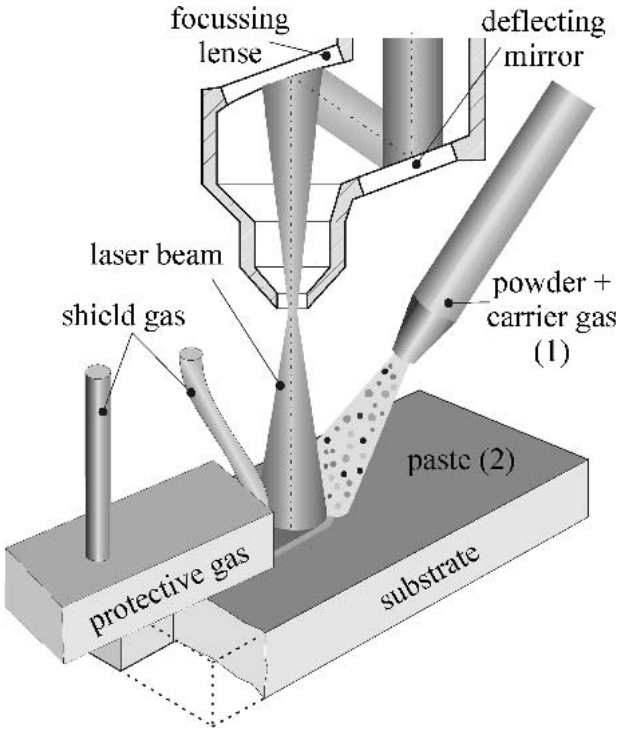

Fig. 2 Sketch of laser processing (1) one-step laser deposition process and (2) two-step laser deposition process

3. Results

For the applied process parameters, a maximum melt depth of about 400 µm was achieved with the CO_2 lasers and about 1000 µm with the Nd:YAG laser. The heat-affected zone was

Table 1 Applied laser process parameters

Parameter	1700 RF	DC 035	DY 044
Laser power, kW	1.3-1.7	2.5-2.8	3.3
Focus distance, mm	5-50	5-45	5-45
Traverse speed, m/s	12-36	60-96	60-120
Track distance, mm	<1.2	<1.5	<3.5
Overlap, %	15-50	15-30	15-30
Shield gas flow (Ar)			
Radially, sLpm	<10	<10	<10
Coaxially, sLpm	<8	<8	<8
Additive	B		
	TiB_2,	TiB_2,	TiB_2,
	ZrB_2,	ZrB_2,	ZrB_2,
	CrB_2	CrB_2	CrB_2
Carrier gas flow, sLpm	<3	Only	Only
Feed rate, g/min	<5	Pastes	Pastes

Table 2 Applied powder size fractions

Material	Size fraction, µm
Boron	<40
TiB_2	<40; <63; <90; <125; <200; >40, <90; >90, <125
ZrB_2, CrB_2	<40; <90; <125; >40, <90

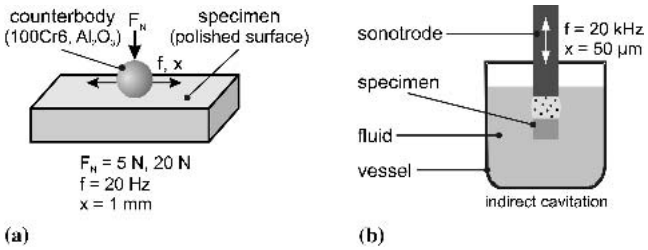

Fig. 3 Schemes of (a) oscillating and (b) cavitation erosion wear tests

400 to 600 μm thick. To ensure a relatively constant thickness of the melt depth during treatment of extended surface areas, a 20 to 35% degree of overlapping of single laser tracks was necessary. Trapping of approximately 50 μm diam gas bubbles in the molten zone near the melt bottom was observed in several cases. Focus distances between +20 and +50 mm are suitable for all applied laser systems to achieve a lens-shaped melt pool cross section. For shorter focus distances, pronounced deep melting on the jet axis occurred, and for longer distances, the remelting depth dropped significantly while the expansion of the heat-affected zone increased. Depending on the applied laser power and traverse speed, the optimum focus distance for maximum molten volume varied between +20 and +35 mm.

In the heat-affected zone, a mixture of a Widmannstätten-like and a martensitic microstructure can be observed (Fig. 4). This can be attributed to a heat treatment at temperatures exceeding the β-phase transition temperature of the alloy (~995 °C) and a subsequent rapid cooling.

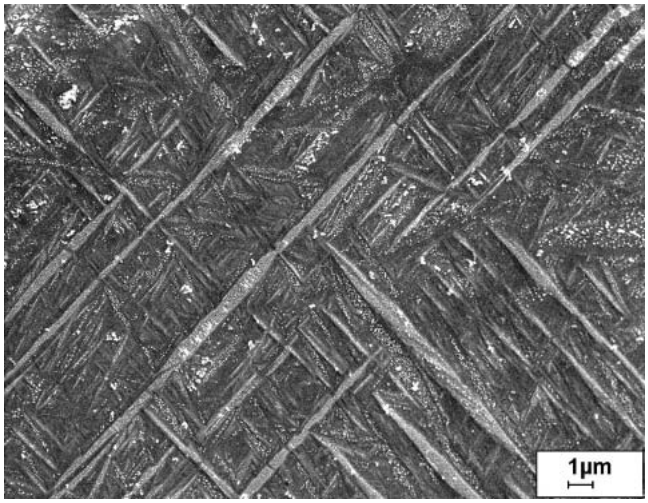

Fig. 4 SEM image of the microstructure of the heat-affected zone

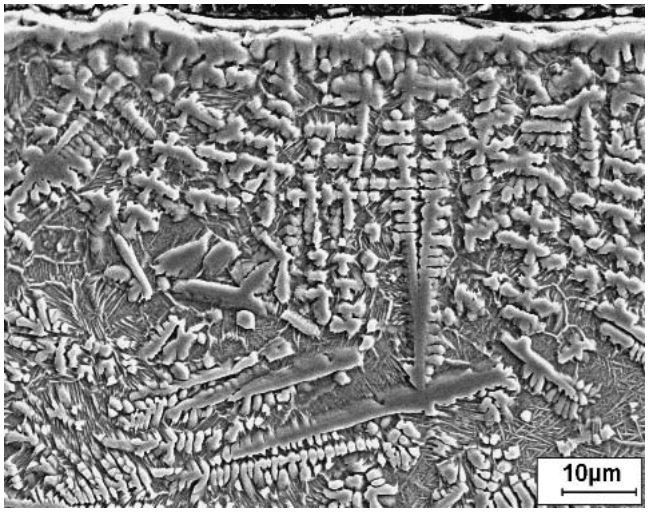

Fig. 5 SEM image of the microstructure of a laser-dispersed Ti6Al4V surface with oxygen admission during the laser treatment

Oxygen entrainment, which cannot be prohibited completely without application of the gas protection setup, results in a mainly dendritic microstructure of Ti, especially near the surface, and was accompanied by oxide-scale formation (Fig. 5). Both for the use of pastes and the injection of powders by a carrier gas, the gas protection setup proved to be suitable to provide an inert atmosphere. The highest content of borides in the laser-treated titanium alloys was achieved by applying pastes. This was because the efficiency of the powder injection into the melt pool by a carrier gas stream is relatively poor.

The microstructure of the metallic matrix in the reinforced surface zone differs scarcely from the heat-affected zone. The state of borides in the laser-treated surface strongly depends on the size of the applied powders. The application of powders of a maximum size of 40 μm resulted in complete dissolution and precipitation of extremely small plates as well as needle-shaped borides. By the use of coarse diboride powders, a particle core can be retained in the initial state. However, diffusion processes lead to a change of the chemical composition and to phase transformation inside the particles. The solution process and the precipitation behavior during solidification were comparable for boron and the diboride powders.

The molten zone has a β-Ti/TiB_x eutectic phase mixture and a very fine lamellar and martensitic α/β-Ti matrix phase mixture, which is formed by transformation from the β-Ti phase. The TiB_x crystals thickness is about 10 nm, and their length usually does not exceed 1 μm (Fig. 6). Their size is too small to permit identification of the boride type either by energy dispersive x-ray spectroscopy (EDXS) or by x-ray diffraction analysis. However, the Ti-B phase diagram (Fig. 1) suggests the formation of TiB for Ti rich regimes.

There is a homogeneous distribution of the eutectic β-Ti/TiB phase mixture inside the molten zone. For relatively low B contents—that is, under eutectic B content—the eutectic phase mixture is arranged like cell walls (Fig. 7). With increasing content of the eutectic phase component, the homogeneity of the molten zones microstructure is improved. At a B concentration of approximately 8 at.% in the molten zone, the microstructure is fully eutectic (Fig. 8). In this case, a microhardness exceeding 610 $HV_{0.05}$ is achieved, which is significantly higher than that of Ti6Al4V in the initial state (350 $HV_{0.05}$).

By application of coarse diboride powders, the solution process can be restricted to a degree that permits embedding of compact particle residues. Despite the diffusion and phase transformation, the embedded particles microhardness exceeds 2000 $HV_{0.05}$. The content of compact particle residues is low, and the distribution is very heterogeneous. Therefore, there is also a strong deviation of the local hardness.

The binder's choice influences the laser dispersing process significantly. The use of Vaseline and PVA resulted in severe crack formation during cooling of the laser-dispersed surfaces (Fig. 9). In the molten zone, a dendritic carbide phase is detected, which can be attributed to binder residues. Pastes with ethanol or PEG permitted production of crack-free boride reinforced surfaces with homogeneous microstructure (Fig. 10). For the application of the PEG binder, a preheating to temperatures of ~230 °C was necessary to achieve well adherent boride particles on top of the Ti6Al4V and complete removal of the binder. The direct laser processing of preheated sheets also proved to be suitable for significant reduction of substrate distortion.

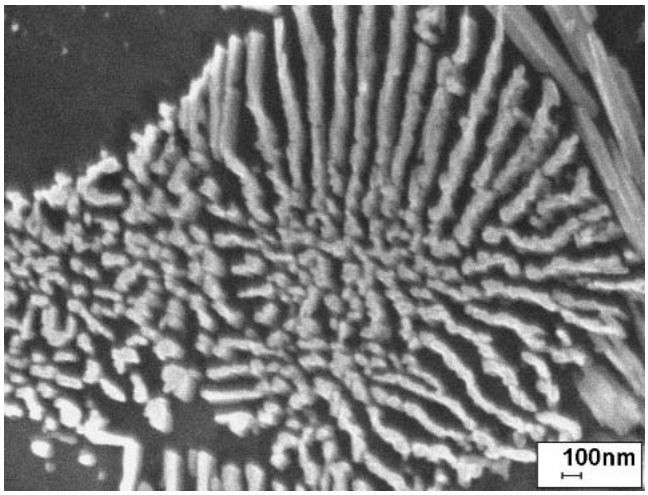

Fig. 6 SEM image of platelike boride precipitates in the β-Ti/TiB eutectic phase

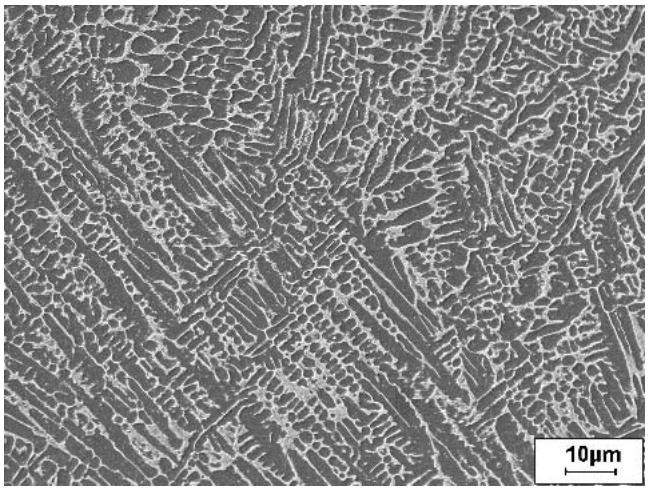

Fig. 7 SEM image of the cell wall arrangement of the eutectic β-Ti/TiB phase mixture in a TiB_2 laser-dispersed Ti6Al4V surface

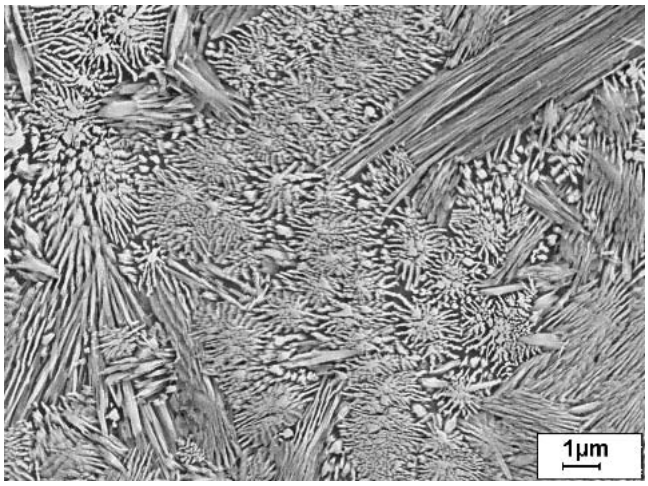

Fig. 8 SEM image of a fully eutectic β-Ti/TiB surface area produced by TiB_2 laser dispersion of Ti6Al4V

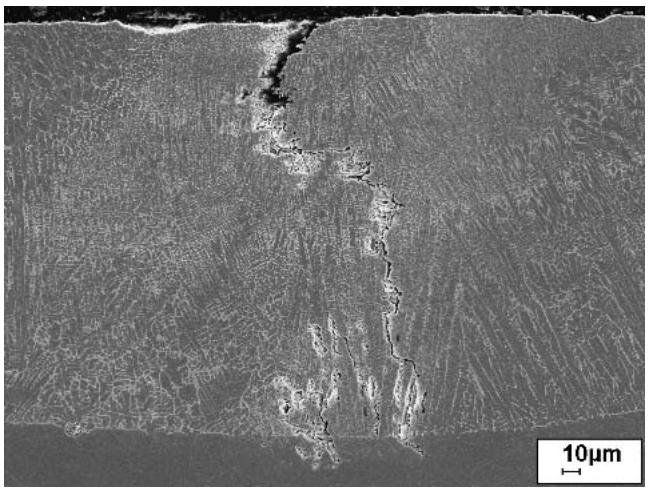

Fig. 9 Crack formation in a modified surface layer after laser remelting with a paste with polyvinyl alcohol binder

The influence of the microstructure on the microhardness is given in Table 3. Martensitic shares in both the pure remelted Ti6Al4V and the heat-affected zone resulted in only slightly increased hardness in comparison to the untreated alloy. Boride precipitation from the alloyed melt permitted an increase of the microhardness up to 610 $HV_{0.05}$ for a fully eutectic composition. Only the embedding of compact boride particles resulted in a significantly enhanced mixed hardness of the boride reinforced Ti6Al4V surfaces.

Though laser dispersing with diborides increases the hardness of Ti6Al4V surfaces significantly and there is a fine microstructure with the TiB hard phase embedded in the ductile metallic matrix, even more severe wear in comparison to untreated surfaces was observed in oscillating wear tests, if there were no diboride particle residues embedded (Table 4). SEM investigations on the worn surfaces proved that the increased wear rate could be attributed to the tribologically induced formation of titanium oxide, which acts as abrasive debris. The extremely fine TiB needles do not resist the exposure to these wear conditions, but form further abrasive debris. However, with rising density of diboride particle residues present at the tested surface, the wear resistance increased significantly. Wear track depth reduction by 40% in comparison to untreated Ti6Al4V is possible. Within the applied condition limits, the described coherences depend neither on the counterbody material nor on the applied load.

In cavitation erosion wear tests, generally a significantly improved wear resistance of the surface layers modified by laser dispersion with diborides was observed (Fig. 11). In contrast to the oscillating wear test, the best performance was achieved for completely dissolved diboride particles. In comparison to the untreated TiAl6V4, the mass loss is decreased by 70%. Modified surface layers with inclusion of diboride particle residues are somewhat inferior in performance, yet the mass loss is 65% lower compared with untreated TiAl6V4.

The excellent corrosion behavior of TiAl6V4 is not affected significantly by laser dispersion of borides either for fully dissolved diborides or for surface layers containing diboride par-

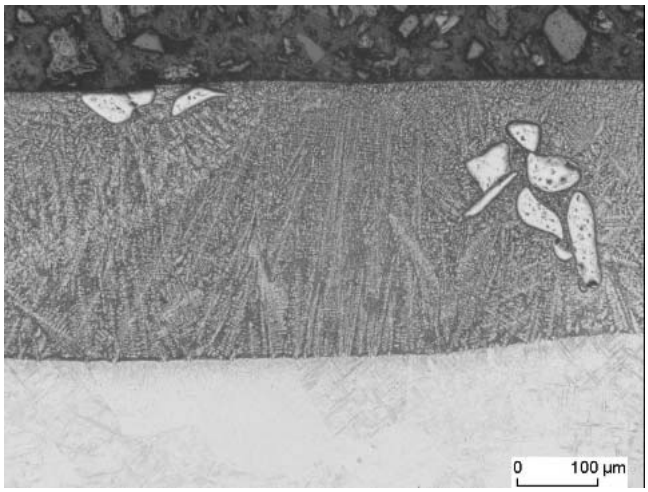

Fig. 10 Crack-free TiB_2 laser-dispersed Ti6Al4V surface with a paste with PEG binder applied

Table 3 Microhardness depending on the microstructure

Microstructure	Microhardness, $HV_{0.05}$
Initial Ti6Al4V	350-360
Remelted Ti6Al4V	390
Heat-affected Ti6Al4V	390
Fully eutectic Ti-TiB phase	610
Compact boride particle residues	2000-3000

Table 4 Oscillating wear test results

Microstructure	Wear track depth, µm	Wear track width, µm
Initial Ti6Al4V (bimodal)	85	2130
Ti6Al4V remelted	60	1795
TiB reinforced Ti6Al4V	88-97	1875-1980
TiB reinforced Ti6Al4V + low density TiB_2	77	1775
TiB reinforced Ti6Al4V + high density TiB_2	50	1640

Note: counterbody: Al_2O_3 ball, 9 mm diameter; load: 5 N; 18,000 wear cycles

ticle residues (Ref 22). For dispersion of diborides, generally a shift of about 100 mV toward more noble standard potentials is observed, which indicates a decreased tendency to corrosion. While modified Ti6Al4V surfaces containing ZrB_2 show almost identical current densities to Ti6Al4V in the initial state in the anodic part of the curve, dispersion of TiB_2 results in increased current densities (Fig. 12). However, the increase is rather small. The worst performing specimens, which have been dispersed with very coarse TiB_2, show an increase of current density by roughly one order of magnitude.

The protective gas setup used is suitable only for one-step laser dispersing of flat surfaces and by use of an additional apparatus, cylindrical components can be reinforced. Dispersing of component surfaces with complex dimensions is possible only by two-step laser deposition, as entrainment of atmospheric gases due to turbulences of carrier and protective gas streams

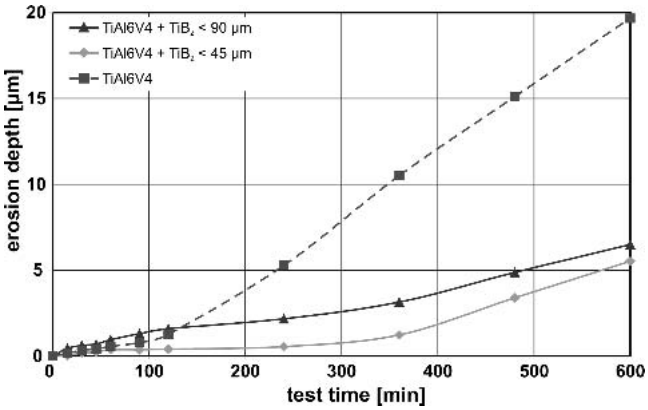

Fig. 11 Influence of TiB_2 laser dispersion on the cavitation erosion wear behavior of Ti6Al4V

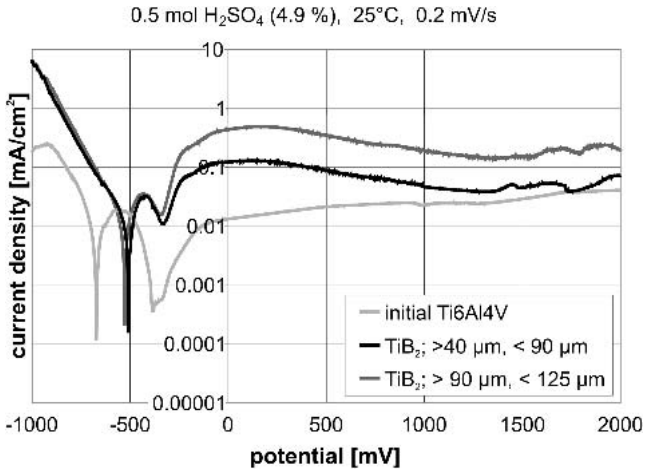

Fig. 12 Influence of TiB_2 laser dispersion on the corrosion behavior of Ti6Al4V

cannot be avoided securely. To achieve a homogeneous microstructure of modified Ti alloy surfaces by two-step laser deposition, a defined amount of hard phases needs to be deposited with homogeneous distribution. The use of pastes does not fulfill these demands for complex-shaped components. Vacuum plasma spraying was carried out to prove the applicability for deposition of thin diboride coatings with homogeneous thickness distribution on Ti6Al4V components. First TiB_2 coatings, which have been manufactured by vacuum plasma spraying, show very high porosity. Optimization of process parameters is necessary.

4. Conclusions

Ti6Al4V surfaces have successfully been reinforced by diborides using one-step and two-step laser deposition processes. For reliable processing, the use of a protective gas setup with inert atmosphere protecting the treated surface zones is required. B and diborides rapidly dissolve in the Ti6Al4V melt, which results in precipitation of extremely fine TiB during cool-

ing. The use of coarse diboride particles permits the embedding of partially undissolved particles. The microhardness of the eutectic β-Ti/TiB phase mixture exceeds 600 $HV_{0.05}$. Locally, significantly higher values are achieved by the embedding of compact boride residues. The application of pastes is advantageous with regard to the efficiency of feedstock incorporation. Different paste binders were tested. Ethanol and polyethylene glycol proved to be suitable to produce crack-free boride reinforced TiAl6V4 surfaces with a homogeneous microstructure.

Only for embedding of diboride particle residues, which is achieved for application of powders with diameters exceeding 45 μm, is the oscillating wear resistance improved in comparison to untreated TiAl6V4. For optimized resistance, the amount and the distribution homogeneity of the diboride particle residues need to be improved. In contrast, for cavitation erosion wear conditions, complete dissolution of the diboride feedstock results in the lowest wear. The mass loss can be reduced by 70%.

Further investigations will be carried out on the optimization of the content and homogeneity of the distribution of undissolved diboride particle cores in the remelted zone to optimize the microstructure of the modified surface layers especially for oscillating wear conditions. Local preheating by use of beam splitters will be applied to minimize residual stresses.

Acknowledgments

The authors gratefully acknowledge financial support from the German Federal Ministry of Economic and Employment Affairs BMWA (AiF 12.643 B) for this research work. Also, the authors thank Wacker Ceramics GmbH, Kempten, Germany, for providing diboride powder with various size fractions. Additionally, the authors would like to thank the Institute of Production, Engineering and Welding Technologies Halle (SLV Halle Ltd.) for providing the slap laser DC 035 and the Nd:YAG DC 044 laser.

References

1. U. Wiklund and I.M. Hutchings, Investigation of Surface Treatments for Galling Protection of Titanium Alloys, *Wear,* Vol 250/251 (No. 2), 2001, p 1034-1041
2. J. Senf, G. Berg, C. Friedrich, E. Broszeit, C. Berger, F. Stippich, P. Engel, and G.K. Wolf, Capability of PVD-CrN Coatings on Light Weight Alloys, *Mater. Sci. Eng. Technol.,* Vol 29 (No. 1), 1998, p 9-15 (in German)
3. A.F. Azevedo, E.J. Corat, N.F. Leite, and V.J. Trava-Airoldi, Chemical Vapor Deposition Diamond Thin Film Growth on Ti6Al4V Using the Surfatron System, *Diamond Relat. Mater.,* Vol 11 (No. 3-6), 2002, p 550-554
4. E. Zeiler, "CVD Diamond Coatings on Titanium Turbine Blades for Improved Oscillating Wear Resistance," Ph.D. Dissertation, University of Nürnberg-Erlangen, Germany, 2001 (in German)
5. D. Muster, A. Makram-Hage, K.T. Rie, T. Stucky, A. Cornet, and D. Mainard, Plasma Deposition, Plasma Coating and Ion Implantation to Improve Metallic Implants and Protheses, *MRS Bull.,* Vol 25 (No. 1), 2000, p 25-32
6. T. Grögler, S.M. Rosiwal, and R.F. Singer, Wear Protection of Titanium Alloys by CVD Diamond Coatings for Aeronautic Applications, *Proc. Materials Week 1998: Materials for Traffic Technology* (Munich, Germany), Vol 2, Wiley-VCH, 1 Weinheim, Germany, 1999, p 503-508 (in German)
7. B.S. Yilbas, A. Coban, A. Kahraman, and M.M. Khaled, Hydrogen Embrittlement of Ti-6Al-4V Alloy with Surface Modification by TiN Coating, *Int. J. Hydrogen Energy,* Vol 23 (No. 6), 1998, p 483-489
8. D. Jäger, W. Schlump, and B. Mehren, Phase Evolution During Reactive Plasma Spraying, *DVS-Band 175,* DVS-Verlag, Dusseldorf, Germany, 1996, p 14-18 (in German)
9. E. Lugscheider, P. Remer, H. Reymann, L. Zhao, and R.W. Smith, Shaping by Reactive Plasma Spraying, *DVS-Band 175,* 1996, p 351-353 (in German)
10. E. Lugscheider, H. Jungklaus, L. Zhao, and H. Reymann, Reactive Plasma Spraying of Coatings Containing In Situ Synthesized Titanium Hard Phases, *Int. J. Refract. Met. Hard Mater.,* Vol 15 (No. 5-6), 1997, p 311-315
11. E. Lugscheider, L. Zhao, and A. Fischer, Reactive Plasma Spraying of Titanium, *Adv. Eng. Mater.,* Vol 2 (No. 5), 2000, p 281-284
12. B.L. Mordike, Surface Hardening of Structural Parts, *Proc. LANE 94*, M. Geiger and F. Volletsen, Ed., Meisenbach, Bamberg, 1994, p 227-234
13. K. Wilsdorf and H.-J. Spies, Gas and Plasma Nitriding of the (a + β) Tittanium Alloy TiAl6V4, *Mater. Sci. Eng. Technol.,* Vol. 28 (No. 11), 1997, p 511-519 (in German)
14. B. Brenner, S. Bonss, R. Franke, and I. Haas, Mechanical and Tribological Properties of Laser Gas-Alloyed Ti6Al4V, *Proc. ECLAT 96,* H.-W. Bergmann and F. Dausinger, Materials and Heat Treatment, Germany, 1996, p 477-484
15. S. Bonss, B. Brenner, E. Beyer, Laser Gas Alloying of Titanium, *Mater. Sci. Eng. Technol.,* Vol 32 (No. 2) 2001, p 160-165
16. U.K. Stolz, F. Sommer, and B. Predel, Phase Equilibria of Aluminium-Rich Al-Ti-B-Alloys—Solubility of TiB_2 in Aluminium Melts, *Aluminium*, Vol 71, 1995, p 350-353
17. *Binary Alloy Phase Diagrams,* 2nd ed., ASM International, 1996
18. L. Lecrivain and G. Provost, Properties of PLASMA SPRAYED BORIDES and Nitrides, *Ber. Dtsch. Keram. Ges.,* Vol 45 (No. 7), 1968, p 347-351 (in German)
19. H. Gruner, Possibilities and Limits of the Vacuum Plasma Spraying Technique, *Metalloberfläche*, Vol 40 (No. 12), 1986, p 522-527 (in German)
20. P.V. Ananthapadmanabhan, K.P. Sreekumar, P.V. Ravindran, and N. Venkatramani, Electrical Resistivity of Plasma-Sprayed Titanium Diboride Coatings, *J. Mater. Sci.,* Vol 28 (No. 6), 1993, p 1655-1658
21. G. Kolbe, K.-J. Matthes, B. Wielage, A. Wank, and H. Podlesak, Boride Reinforced Surfaces of TiAl6V4-alloy, *Proc. Materials Week 2002,* DGM, Frankfurt, Chemnitz, Germany, 2002
22. K.-J. Matthes, B. Wielage, G. Kolbe, and A. Wank, "Laser Dispersing of Titanium Alloys for Manufacturing of Boride Reinforced Highly Wear and Corrosion Resistant Surfaces," Final Report of AiF Project 12.643 BR, funded by the German Federal Ministry of Economic and Employment Affairs BMWA, DGM, Frankfurt, Chemnitz, Germany, p 1-61 (in German)